HOKKAIDO UNIVERSITY

Title	Calciothermic reduction of NiO by molten salt electrolysis of CaO in CaCl2 melt
Author(s)	Descallar-Arriesgado, Reyna Famila; Kobayashi, Naoto; Kikuchi, Tatsuya et al.
Citation	Electrochimica Acta, 56(24), 8422-8429 https://doi.org/10.1016/j.electacta.2011.07.027
Issue Date	2011-10-01
Doc URL	https://hdl.handle.net/2115/47442
Type	journal article
File Information	EA56-24_8422-8429.pdf

Hokkaido University Collection of Scholarly and Academic Papers : HUSCAP

Calciothermic reduction of NiO by molten salt electrolysis of CaO in $CaCl_2$ melt

Reyna Famila Descallar-Arriesgado*, Naoto Kobayashi, Tatsuya Kikuchi and Ryosuke O. Suzuki

Division of Materials Science and Engineering, Faculty of Engineering, Hokkaido University, Sapporo 060-8628, Japan

**Corresponding Author. Tel: +81-080-4049-0996; Email: yenyen2day@yahoo.com*

Abstract

Metallic nickel powders with low and uniform residual oxygen content were produced from NiO using the molten salt electrolysis of CaO in $CaCl_2$ melt. Suitable amount of CaO for the reduction was in the range of 0.5 – 3.0 mol% CaO.

The electrical isolation of NiO from both electrodes could produce metallic Ni in $CaCl_2$ melt. Separating the metal oxides from the cathode confirmed the mechanism of calciothermic reduction that the electrolysis of dissolved CaO in $CaCl_2$ melt produces Ca, and that the dissolved Ca in molten $CaCl_2$ successfully reduces NiO to metallic Ni. An average of about 600 ppm oxygen in Ni sample was achieved directly from oxide, when NiO was detached from the cathode.

Keywords: Nickel oxide, calcium oxide, calcium chloride, calciothermic reduction, molten salt electrolysis

1. Introduction

A direct way of oxide reduction by using molten salt electrolysis has been intensely investigated for the past decade. Metal oxides are immersed into a bath of molten salt and electrolyzed by applying electric field. The metallic products are formed at the cathode and the carbonic gases are expelled at the anode [1-13]. Aside from pure metal production, this process was tried in producing some alloys and intermetallic compounds directly from the oxide mixture [14-19], making it an attractive reduction method. Varieties of salts are employed as the electrolytes, but the salt most largely used is $CaCl_2$-based salt because calcium chloride can dissolve up to 20 mol% CaO [20-22] and because a small addition of CaO in $CaCl_2$ was found to improve the rate of reduction and deoxidation [3-9,12,13].

Two notable yet conflicting ideas on the effect of calcium oxide addition to the molten salt were presented by the OS process and FFC-Cambridge process.

Calcium chloride can dissolve 2 to 4 mol% Ca at 1173 K in equilibrium [23-28]. OS process speculated that the presence of Ca dissolved in molten salt was responsible for reduction [1-9]. The dissolved Ca reacts with titanium dioxide producing metallic titanium and CaO as presented in Eq.1 [1-3]. When an electric field is applied between the two electrodes, the electrolysis of CaO occurs to produce Ca near the cathode and at the same time two carbonic gases are produced at the anode as shown by Eqs.3 and 4, respectively. CaO becomes the source of Ca for the calciothermic reduction of metal oxide in molten $CaCl_2$ and for the further deoxidation (Eq.1 & 5), producing a highly reduced metal with low residual oxygen.

$TiO_2 + 2\underline{Ca} = Ti + 2\underline{CaO}$ (reduction) (1)

$\underline{CaO} = Ca^{2+} + O^{2-}$ (2)

$Ca^{2+} + 2e^- = \underline{Ca}$ (at cathode) (3)

$O^{2-} + C = CO_n + 2ne^-$ (n=1 or 2) (at anode) (4)

$\underline{O}$(in Ti) + Ca = $\underline{CaO}$ (deoxidation) (5)

FFC-Cambridge process [10-19], on the other hand, is considered as the concept of cathodic oxygen ionization of the solid oxide in the molten salt to reduce the pelletized metal oxide precursor which is served as the cathode (Eq.6). FFC-Cambridge cathodic reaction is presented by the following equations [10]:

$TiO_2 + 4e^- = Ti + O^{2-}$(in $CaCl_2$) (electro-reduction) (6)

$\underline{O}$(in Ti) + $2e^- = O^{2-}$(in $CaCl_2$) (electro-deoxidation) (7)

It was asserted that a moderate concentration of CaO promotes the better reaction rate due to the enhanced oxide ion transfer across the electrolyte [12,13]. CaO content in the electrolyte is a key parameter to the process. FFC mechanism argued that the presence of dissolved Ca in the electrolyte causes an undesired side effect because it imparts a degree of electronic conduction on the electrolyte and lowers current efficiency [11, 13]. Therefore, Ca is not a requirement for reduction in FFC mechanism.

The proper CaO concentration suitable for reduction has been rarely investigated, despite the fact that calcium oxide addition to molten calcium chloride yields positive results. Namely, in the purely calciothermic reduction of TiO_2 without external electrochemical potential [3], 0.5 mol% CaO in the $CaCl_2$ melt resulted to the better deoxidation, i.e., the lowest residual oxygen in the reduced metallic titanium was

achieved. Therefore, it has often taken as the standard condition in CaO concentration [4-9]; however, no experimental optimizations have been given in the concept of OS process. This work aims to examine the CaO concentration that is favourable for reduction and deoxidation of metal oxide in the case of electrolysis in the molten $CaCl_2$ bath.

This work will also characterize OS process from FFC-Cambridge process to prove the calciothermic reduction and deoxidation by electric isolation of the metal oxide from the cathode during electrolysis. In TiO_2 reduction, the complex oxides such as $CaTiO_3$ and Ca_2TiO_4 were often formed as the intermediate phases during reduction to pure metallic titanium [3-13], and these formations disturbed the detailed analysis on the CaO concentration suitable for reduction. Nickel oxide was used in this work because it was found in the preliminary experiments [9] that nickel oxide did not lead to the formation of any complex oxides, alloys or intermetallic compounds with calcium when NiO was reduced in molten $CaCl_2$. In their paper, Yan and Fray, also produced metallic nickel directly from the oxide with no other lower oxides or Ca-Ni alloys by-product. Detailed analysis on NiO reduction using molten salt electrolysis however has not been reported.

When NiO is in physical contact with C, solid state carbothermic reduction may occur at 1173K (ΔG^o = -128.9 kJ mol^{-1}[29]). However, it was reported that the carbothermic reduction was very slow at 1173K; for instance only 30% reduction after 6 hours [30]. This work excludes any possibility of carbothermic reduction; there was no physical contact between the oxides and carbon in molten $CaCl_2$.

When NiO was mixed with another oxide such as TiO_2, CeO_2 or MgO, it was reported that NiO was preferentially reduced to nickel metal before the reduction of Ti,

Ce or Mg oxide, respectively, in the $CaCl_2$ melt [15-19]. This indicates that the thermodynamic stability of NiO is not as strong as compared with the other oxides. It is proved thermodynamically that the oxygen potential of NiO is higher than those of the other oxides. Thus, NiO was a suitable oxide to study the initial stage of reduction in the molten $CaCl_2$.

2. Experimental

Six hundred grams of anhydrous $CaCl_2$ (>95%, Wako Chemical Co.) was mixed with CaO (99.9%, Kanto Chemical) calcined in air, and used as electrolyte by filling inside a magnesia crucible (Fig. 1). A basket-like cathode was prepared by wrapping two nickel disks (15 mm in diameter, a few mm thick) doubly in Ni net (150 mesh). 1.5g of nickel monoxide (>99%, Wako Chemical Co.) was loosely poured inside the cylindrical basket. The basket was connected to a stainless steel rod as shown in Fig.1. A graphite electrode (10 mm in diameter) was used as the anode. The electrodes were attached to the cover of stainless steel vessel using silicone stopper, and a distance of about 20 mm between the anode and cathode was maintained throughout all the experiments.

The magnesia crucible was heated slowly in vacuum to 873K. This condition was maintained at this temperature for at least 36 ks to ensure that any hydrates will be completely decomposed and the moisture in the vessel removed. After moisture removal, argon gas was charged into the vessel. The temperature was gradually raised to 1173K for 10.8 ks in Ar gas environment and allowed to stabilize for 1.8 ks. The electrodes were submerged into the salt bath at the depth about 10 mm above the bottom of the crucible. A constant voltage of 3.1V was then applied to the electrodes. Current between

the two electrodes were recorded every 5s. After 1.8 ks, power supply was terminated and the electrodes were pulled up to the upper part of the vessel. The furnace was then cooled-down to room temperature.

The basket-like cathode was taken out of the furnace, washed with distilled water and then placed in an ultrasonic vibration cleaner. The slightly sintered sample was taken out of the Ni basket and carefully sliced into 3 parts with approximately 2.5 mm circumferential interval from the Ni net where the sample attached. These 3 parts were then separately crushed into fine grains. In order to remove the solidified salt residue from the specimens completely, the samples were again washed by distilled water, acetic acid, distilled water, ethanol and acetone in exact order. The specimens were then dried in vacuum. Phases were examined using X-ray diffraction (XRD) analysis. Residual oxygen content was determined by the inert gas fusion-infrared adsorption method using LECO TC600 oxygen/nitrogen analyzer. Morphologies of the resulting powders were observed under the scanning electron microscope (SEM).

3. Results and discussion

3.1 Concentration dependency of the current

A constant voltage of 3.1 V between two electrodes was applied in all the electrolysis. Except for CaO concentration, all the other experimental conditions were the same for all the runs. For example, the quantity of NiO, the distance between the two electrodes, electrolysis time, holding temperature and applied voltage were set as the same for all experiments.

In OS mechanism, the theoretical charge, Q_o, is defined as the charge required to generate stoichiometric amount of Ca reductant for the reduction of the filled amount of NiO. On the other hand, Q_o, is also defined as the theoretical charge for oxygen ion

removal from the served oxide pellet in case of FFC mechanism. Thus the defined Q_o are identical. The supplied charge, Q, was calculated by integrating current with respect to time. Consequently, the ratio of Q/Q_o is used as normalized parameter for the amount of supplied electric charge.

Table 1 listed the calculated Q/Q_o at various CaO concentrations electrolyzed for 1.8 ks at 1173 K. After 1.8 ks electrolysis, the supplied charge already exceeded 100% for all experiments. Q/Q_o increased with increasing CaO concentration, denoting that the oxide ion transfer is enhanced at higher CaO concentration in the FFC concept. Increase of Q/Q_o also indicates in the framework of OS process that the larger amount of Ca per time was produced at the higher CaO concentration.

Time dependency of current was recorded from the start to the end of electrolysis with 5 s interval, as shown in Fig. 2. High initial current peaks are observed in the electrolysis at various CaO concentrations. According to the work of Schwandt and Fray [11], for a dilute electrolyte (i.e. $CaCl_2$-0.2 mol% CaO) with two electrode terminals, this initial current peak is due to the incorporation of calcium ions into the cathode. Fig. 2 also shows that the current peak is higher at the higher CaO concentration. Fig. 3 graphed the current measured for 5 s after the start of electrolysis as a function of CaO concentration. This current increased, as CaO was added to the electrolyte until it reaches a plateau at 3.0-5.0 mol% CaO. Obviously, the increase in onset current with the increase in CaO concentration means that the larger amount of Ca species are being generated in the electrolyte with the higher CaO concentration.

Fig. 3 also shows the rate of current decline as a function of CaO concentration. The rate of current decline was calculated from the slope of the linear regression of current-time curve in Fig. 2. The rate of current decline increased as CaO was added to

the electrolyte up to 3.0 mol%, and slightly dropped when CaO content increased to 5.0 mol%. This implies that the rate of reduction was faster at the higher CaO concentration, probably because the larger amount of CaO in the melt was consumed for electrolysis and the larger amount of Ca for reduction is being generated in a short period. Slight decrease in the rate of current decline at 5.0 mol% CaO may be due to the possible precipitation of liquid Ca metal because molten $CaCl_2$ can only dissolved up to 4 mol% Ca [23-28] and this value decreased with small addition of CaO in the bath [31].

3.2 Reduction/deoxidation at various CaO concentration

3.2.1 Morphology

Fig. 4 shows the SEM image of the starting NiO particles and the resulting powder of run 3 taken near the surface of the Ni net. Fig. 4 (a) shows that the starting NiO powder, consisted of fine spherical particles with loose morphology and irregular agglomerates. The average primary particle size is 0.625 μm in diameter obtained by laser light diffraction method. Fig. 4 (b) shows the clustering of Ni grains with individual particle size of about 1-4 μm formed during reduction. This morphology was common in all the powders obtained after 1.8 ks electrolysis. Apparently, during the reduction of NiO, there was grain coarsening. Ni grains of sub-micron sizes were agglomerated into larger chunks of Ni metal, which may trap some unreacted NiO particles. The fast reduction of NiO at the higher CaO concentrations causes a rapid growth of Ni metallic grains, which catches the smaller unreduced NiO particles inside the metallic grain. The traped NiO in the metal is not easy to decompose. Too high rate of reduction may retain some unreacted NiO among large Ni agglomerates.

The microscopic oxygen distribution was tried to be measured by SEM equipped with energy dispersive X-ray (EDX) detector, but the precise profiles were not detected

because of light nature of oxygen. Instead, oxygen distribution in the slightly sintered sample was analyzed with LECO method by separating into 3 parts. It is noted that at least a few hundred milligrams of specimens are needed to obtain the analytical value by this method.

3.2.2 Reduction using pure $CaCl_2$

In order to examine the progress of reduction, the partially sintered powder was sliced into 3 parts to approximately 2.5 mm circumferential interval from the Ni net which the sample attached to. These portions were separately washed, and the phases were identified by XRD measurements as listed in Table 1.

When pure $CaCl_2$ was used as electrolyte, a partial reduction of NiO occurred. The reduction proceeded inward, namely, the NiO particles near the net cathode (0-2.5 mm circumferential distance from the net) was reduced faster than those in the central portion (2.5-7.5 mm circumferential distance from the cathode). An evidence of the partial reduction is the presence of XRD diffraction peaks due to residual NiO in the central part of the cathode.

It may be analyzed that the reduction of NiO was guided by FFC mechanism and can be presented by the following reactions.

At the cathode:

$NiO + 2e^- = Ni + O^{2-}$ (in $CaCl_2$) (electro-reduction) (8)

$\underline{O}$(in Ni) + $2e^- = O^{2-}$ (in $CaCl_2$) (electro-deoxidation) (9)

At the anode:

$$O^{2-} + C = CO_n + 2ne^- \quad (n=1 \text{ or } 2) \quad (10)$$

$$O^{2-} = 1/2O_2 + 2e^- \quad (11)$$

During electrolysis, NiO should be decomposed and reduced into metallic Ni attached to the cathode (Eq.8). The product oxygen ions transfer out of the cathode and flow in the electrolyte. Oxygen ions are attracted to the anode, and react with the graphite electrode to form carbonic gasses as well as oxygen gas if inert anode is used (Eq.10).

Although the decomposition voltage of $CaCl_2$ is about 3.231 V, at almost pure $CaCl_2$ molten salt, chlorine gas evoultion may occur (Eq.12) [11].

$$2Cl^- = Cl_2 + 2e^- \quad (12)$$

$$CaCl_2 = Ca^{2+} + 2Cl^- \quad (13)$$

The decomposition of $CaCl_2$ forms Ca species, which will be attracted in the cathode (Eq. 13). At the first stage of reaction, we need this kind of electrochemical reaction (Eq. 12 & 13), if the electrolyte is completely pure $CaCl_2$. This phenomena the so-called under-potential depostion (UPD), will lead us to Ca formation; then, we can speculate another possible mechanism explaining the NiO reduction through calciothermic reaction.

Even comercially pure $CaCl_2$ was carefully used, contamination with water during handling is possible. Once a faint amount of O^{2-} is supplied to the melt, we cannot distinguish it from O^{2-} in CaO. When Ca^{2+} attracts to the cathode, it is reduced to its metallic state if the condition matches (Eq.14). Ca is soluble in $CaCl_2$, and has

very high reducing ability. This dissolved Ca which is formed on the cathode will chemically react with NiO and reduce it to metallic Ni (Eq.15 & 16). This mechanism is referred to as the OS process and is presented by the following reaction in the case of NiO reduction.

At the cathode:

$Ca^{2+} + 2e- = \underline{Ca}$ (14)

$NiO + \underline{Ca} = Ni + \underline{CaO}$ $\Delta G^{o}_{1173K} = -378.18\ kJmol^{-1}$[29] (reduction) (15)

$\underline{O}$(in Ni) + Ca = $\underline{CaO}$ (deoxidation) (16)

$\underline{CaO} = Ca^{2+} + O^{2-}$ (decomposition) (17)

Anodic reactions are similar with Eqs. 10 and 11. The chemical reaction between NiO and dissolved Ca produces a CaO by-product (Eq.15). This CaO dissolves in the $CaCl_2$ melt and decomposed (Eq.17) spontaneously in the system since the theoretical decomposition voltage of CaO into Ca and O_2 is only 2.652 V [29], much lower than the applied voltage of 3.1 V in the experiment. It will provide a continuous supply of Ca until the reduction of NiO is completed.

The oxygen content in the samples electrolyzed for 1.8 ks is presented in Fig. 5. When pure calcium chloride was used without CaO addition, the oxygen concentration in the sintered product was high and not homogeneous; oxygen concentration was low at the area near the cathode surface, increased slightly at the middle part and raised sharply at the central part of the sintered product. This high oxygen concentration is due to the presence of small amount of unreacted NiO particles, as identified by XRD

analysis. Electrolysis was terminated in 1.8 ks, and this short electrolysis may not be enough to completely reduce the charged amount of NiO when pure $CaCl_2$ was used as electrolyte.

3.2.3 Reduction at 0.5-3.0 mol%CaO

Addition of intermediate amount of CaO significantly improves the reduction of NiO. At $CaCl_2$-0.5 mol% CaO for example, the number of NiO peaks detected by XRD measurement decreased as listed in Table 1. The powders containing a single phase of Ni were achieved at runs 3 and 5, where 1.0 and 3.0 mol% CaO were added to $CaCl_2$, respectively. This proved that the reduction was enhanced by the small addition of CaO.

Small traces of XRD diffraction peaks due to NiO were detected at the innermost portion of the sintered product when the bath containing 2.0 mol% CaO was used, although the samples obtained from the salt with 1.0 and 3.0 mol% CaO completely transformed to the single phase of Ni. The reason of the existence of unreacted NiO in run 4 is still not clear, but the strange rise and fall of current were observed for the span of 1.8 ks, as shown in Fig. 2. The wavy behaviour of the current during electrolysis may reflect an unstable nature in this condition.

Better reduction can be observed also in Fig. 5. Oxygen distributions in the sintered sample showed homogeneous trend when 0.5-3.0 mol% CaO was added to $CaCl_2$. When CaO is added in the salt up to 3 mol%, the oxygen contents became smaller compared with the oxygen content when no CaO was added in $CaCl_2$ electrolyte, although electrolysis time was the same. When $CaCl_2$ - 0.5-3.0 mol% CaO was used,

more uniform profile in oxygen concentration was achieved, and the residual oxygen at the central part of the sample decreased.

The improvement of reductions, i.e., the lowering of oxygen concentration in the resulting product, might be explained by FFC mechanism. FFC-Cambridge process claimed that, when using $CaCl_2$ with very low CaO concentration, the oxygen transport across the electrolyte is limited, resulting to slow electro-reduction and sluggish electro-deoxidation [11-13]. When an intermediate amount of CaO is added in $CaCl_2$ such as 2.0 mol% CaO, however, the ability of the electrolyte to transport oxide ions was enhanced leading to a better reaction rate [12, 13]. Thus, in FFC mechanism, the addition of CaO in the $CaCl_2$ bath is important for improved reduction.

Otherwise, the better reduction and deoxidation at the higher CaO concentration may be also explained by OS process [1-9]: when CaO is initially added to the salt, it will decompose and generate larger amount of Ca reductant during electrolysis (Eq. 17) than that generated when using pure $CaCl_2$. Decomposition and regeneration of CaO will continuously supply Ca reductant for further reduction and deoxidation (Eqs.15 & 16). The more homogeneous oxygen concentration from the surface to the center of the sintered product can be achieved if the dissolved Ca for NiO reduction was supplied adequately in the central part.

3.2.4 Reduction at $CaCl_2$ – 5.0 mol%CaO

When 5.0 mol% CaO was added to $CaCl_2$, a small amount of NiO remained after the electrolysis as listed in Table 1. After 1.8 ks, the reduction at $CaCl_2$ – 5.0 mol% CaO was clearly incomplete, although the supplied current was high and Q/Q_0 was

enough large. Moreover, the oxygen concentration profile in the sample became inhomogeneous, and a fairly large amount of oxygen remained at the central portion of the sample. The incomplete reduction at $CaCl_2$ – 5.0 mol% CaO can be well explained by two ways following OS mechanism. One explanation is the delayed dissolution of CaO back to the bulk. Another explanation is the precipitation of liquid Ca outside of the cathodic basket. These two possibilities will be explained as below.

Although the CaO saturation is about 20 mol% CaO in CaO-$CaCl_2$ binary system [20-22], it was reported that it took longer time to achieve equilibrium at higher CaO concentration [25, 31]. When the concentration of CaO in the bath is high, the larger current can be supplied; the larger amount of Ca is generated per unit time as explained in section 3.1. It may be assumed that these huge amount of Ca produced reacts with NiO at the same short time, which rapidly produces the high local concentration of freshly formed CaO inside the cathodic basket. This phenomenon may increase the thickness of the boundary layer between the cathode surface and the molten salt. Thickened boundary layer will delay the dissolution of CaO back to the bulk of solution and will also delay the flow of Ca species towards the cathode. Thus, the partially reduced sample inside the cathode is not exposed by the fresh reductant, the extra amount of CaO becomes piled up in the basket-type cathode, and the NiO reduction is slowed-down.

Unfavourable condition at the higher CaO concentration would show another explanation on the possibility of Ca liquid precipitation. As soon as 5.0 mol% CaO is electrolysed in the $CaCl_2$ bath, it will produce a tremendously large amount of Ca in a short period because of high current supply, and locally reaches the solubility limit of

Ca in $CaCl_2$ which is about 4 mol% Ca at 1173 K [23-28]. It is noteworthy that the solubility of Ca rapidly decreases when a small amount of CaO co-exists in the $CaCl_2$ bath [31]. Therefore, the $CaCl_2$ close to the cathode saturates with Ca, and liquid Ca may start to precipitate. These Ca liquid droplets are often called as “metal fog” i.e., in alumina electrolysis and it may deposit on the outer surface of the basket-type cathode. The precipitates that deposit outside of the basket will not be able to reach the NiO filled inside the basket-like cathode, making the reduction ineffective.

These two possible mechanisms suggest that CaO concentration should be limited to an intermediate value, such as 0.5-3.0 mol% CaO, for more efficient reduction.

3.3 Confirmation of calciothermic reduction/deoxidation

Nickel oxide powder used at the preceding experiments was incorporated inside the basket-like cathode made of metallic Ni net. It was assumed that the cathode ionization occurs when metal oxide was electrically connected with the cathode, as FFC process claimed. To avoid ionization and to confirm the mechanism of calciothermic reduction and deoxidation, an independent work was conducted by isolating NiO from the cathode.

Two alignments in the cathode isolation experiments labelled run I-1 and run I-2 are shown in Fig. 6 (a) and (b), respectively. In run I-1, NiO powder was packed loosely inside the nickel basket which was positioned between the graphite anode and nickel platy cathode of 65 mm x 65 mm in dimension. The Ni net was used as the cathode and

it was attached to stainless steel rod by tying it using a thin Ni wire, as shown in Fig. 6 (a).

In run I-2, a small nickel basket of 15 mm diameter was fabricated and NiO powder was filled loosely inside it. The nickel basket was mounted securely at the center of a 22 mm diameter mullite pellet and a nickel net was wrapped around this ceramic pellet. The nickel net was attached to a stainless steel rod current connector, but the inner basket was electrically isolated from the current lead.

The same procedure as mentioned in the experimental section was followed with a salt bath of $CaCl_2$-0.5mol% CaO. The electrolysis time was extended to 10.8 ks. After electrolysis, the sample was pulled out from the bath and the furnace was allowed to cool to room temperature. The resulting slightly sintered powders after both runs were parted in two to test the homogeneity of reduction. For run I-1, the sample was split; one part was the side faced to the cathode, and another part faced to the anode as presented as (x) and (y), respectively, in Fig. 6 (a). For run I-2, the sample was sliced to separate the outer section (near the surface of the Ni basket) and the inner section (the central part of the Ni basket). The pieces of the products were separately washed and phases were identified by XRD.

X-ray diffraction patterns for run I-1 and run I-2 are shown in Fig.7. Only single phase was detected in all the portions. This means that the reduction was completed after both isolation experiments. When the NiO powder was electrically isolated from the current leads, then only calciothermic reduction should occur through the chemical reaction between the dissolved Ca and the submerged NiO in the electrolyte (Eq.15). This proved that the electrolysis to generate Ca from the CaO dissolved in $CaCl_2$ (Eq.

17) was favoured at a voltage higher than the required theoretical voltage to decompose CaO, and that the calciothermic reduction of metal oxide was preferred.

Oxygen content of the powders was examined by LECO oxygen analyzer. Table 2 shows results when NiO was electrically isolated from the cathode. Both isolation experiments showed almost uniform residual oxygen from the two partitions, 568 and 597 ppm for run I-1, and for run I-2, 713 and 749 ppm. This means that the concentration of dissolved Ca in the $CaCl_2$ melt was almost uniform anywhere in the basket.

Scanning electron microscopic image of the samples taken from both runs are shown in Fig. 8, and it is observed that they have similar morphology to that shown in Fig. 4, in which all particles of Ni clustered into larger chunks. These results confirm that the chemical reduction with NiO in the molten salt at 3.1 V was preferentially calciothemic. Obviously, since there was no electrical connection between the NiO and cathode, the presence of dissolved Ca in $CaCl_2$ bath was responsible for the reduction and deoxidation of the metal oxide.

Although using the isolation set-up could successfully reduce NiO, the authors still recommend using the typical set-up in OS process (Fig. 1) for the more efficient electrolysis and the easier positioning between the electrodes and oxides in the salt bath. Integrating the oxides inside the basket-like cathode is still cheaper because it eliminates the use of additional materials such as Ni plate or mullite pellet. In addition, the ease of positioning the typical OS process set-up has greater advantage over the isolation set-up.

4. Conclusions

The electrolysis of CaO in $CaCl_2$ molten salt could reduce NiO powder to form metallic Ni. By increasing the concentration of CaO up to 3.0 mol%, the partially sintered pellet with a single phase Ni was obtained with more homogeneous residual oxygen concentration. Current supplied is relative to the concentration of calcium oxide in the bath. The experiments isolating the nickel oxide from the cathode could confirm the calciothermic reduction and deoxidation through the electrolysis of CaO in $CaCl_2$ molten salt.

Acknowledgements:

The authors would like to Mr. Nobuyuki Miyazaki for his assistance in SEM observation, and Dr. Tatsuhiro Shigyo at Hokkaido Research Organization in NiO particle analysis. This work was financially supported in part by Grants-in-Aid for Scientific Research from the Japan Society for the Promotion of Science (#20360341 and #21656193) and The light Metal Educational Foundation. One of the authors (RFDA) is grateful to MEXT scholarship grant.

References

[1] K. Ono, R.O. Suzuki, JOM, Feb. (2002) 59

[2] R.O. Suzuki, K. Ono, Proc. of the 13th Int. Symp. on Molten Salt, The Electrochem. Soc. , Penningston, NJ (2002) 810

[3] R.O. Suzuki, S. Inoue, Metall. Mater. Trans. B 34 (2003) 277

[4] R.O. Suzuki, K. Teranuma, K. Ono, Metall. Mater. Trans. B 34 (2003) 287

[5] K. Ono, R.O. Suzuki, Proc. Yazawa Int. Symp., Metall. Mater. Processes: Principles And Technique – The Min. Aqueous and Electrochem. Processing vol.III, Minerals, Metals & Materials Soc, OH, USA, (2003) 187

[6] R.O. Suzuki, S. Fukui, Mater. Trans. 45 (5) (2004) 1665

[7] R.O. Suzuki, J. Phys. Chem. Solids 66 (2005) 461

[8] K. Kobayashi, Y. Oka, R.O. Suzuki, Mater. Trans. 50 (2009) 2704

[9] R.O. Suzuki, Proc. of an Int. Symp., Processing and Fabrication of Advanced Materials -XVIII, Sendai, Japan 18 (2009) 701

[10] G.Z. Chen, D.J. Fray, T.W. Farthing, Nature 407 (2000) 361

[11] C.Schwandt, D.J. Fray, Electrochim. Acta 51 (2005) 66.

[12] C.Schwandt, G. T.L. Alexander, D.J. Fray, Electrochim. Acta 55 (2009) 3819

[13] C.Schwandt, G. R. Daughty, D.J. Fray, Key Eng. Mater. 436 (2010) 13

[14] X.Y. Yan, D.J. Fray, Min. Processing Extr. Metall., Trans. Inst. Min. Metall. C 116 (1) (2007) 17

[15] B. Jackson, M. Jackson, D. Dye, D. Inman, R. Dashwood, J. Electrochem Soc. 155 (2008) 171

[16] Y. Zhu, M. Ma, D. Wang, K. Jiang, X. Hu, X. Jin, G.Z. Chen, Chin. Sci. Bulletin 51 (20), (2006) 2535

[17] B. Zhao, L. Wang, L. Dai, G. Cui, H. Zhou, R.V. Kumar, J. Alloys Compd. 468, (2009) 379

[18] S. Tan, K. Aydinol, T. Ozturk, I. Karakaya, J. Alloys Compd. 504, (2010) 134

[19] S. Jiao, L. Zhang, H. Zhu, D.J. Fray, Electrochim. Acta 55, (2010) 7016

[20] B. Neumann, C. Kroeger, H. Juettner. Z. Elektrochem. 41 (10) (1969) 725

[21] D.A. Wenz, I. Johnson, R.D. Wolson, J. Chem. Eng. Data 14 (2) (1969) 250

[22] G.S. Perry, L.G. MacDonald, J. Nucl. Mater. 130 (1985) 234

[23] D.T. Peterson, J.A. Hinkebein, J. Phys. Chem. 63 (1959) 1360

[24] R.A. Sharma, J. Phys. Chem. 74 (22) (1970) 3896

[25] V. Dosaj, C. Aksaranan, D.R. Morris, J. Chem. Soc. Farraday Trans. 71 (1975) 1083

[26] H. Fishnach, Steel Res. 56 (7) (1985) 365

[27] L.-I. Staffansson, D. Sichen, Scand. J. Metall. 2 (1992) 165

[28] A.I. Zaitsev, B.M. Mogutnov, Metall. Mater. Trans. B 32 (2001) 165

[29] A. Roine, “HSC Chemistry”, ver.6.12, Outotec Res. Oy, Pori, Finland (2007)

[30] S.K. Sharma, F.J. Vastola, P.L. Walker, Jr., Carbon 35 (4) (1997) 535

[31] K.M. Axler, G.L. DePooter, Mater. Sci. Forum, 73-75 (1991) 19

Table and Figure Captions

Table 1. Supplied charge, Q/Q_O, and phases identified by XRD when the samples were electrolyzed for 1.8 ks at 1173 K.

Table 2. Supplied charge, Q/Q_O, and phases identified by XRD when NiO was electrically isolated from the cathode. Electrolysis time was 10.8ks, applied voltage was 3.1 V and electrolysis temperature was 1173K.

Fig 1. Experimental apparatus for electrolysis.

Fig 2. Current versus time curves obtained during electrolysis for 1.8 ks at 1173 K with a constant potential of 3.1 V.

Fig 3. The current reading at the start of electrolysis and the average slope of current decline.

Fig 4. Scanning electron microscopic image of (a) starting NiO particles and (b) the sample reduced in a $CaCl_2$-1.0mol% CaO bath for 1.8 ks.

Fig 5. Oxygen concentration distribution in the partially sintered samples.

Fig 6. Electrodes and NiO position during isolation experiment, (a) for run I-1 where NiO was placed in between the anode and cathode, and (b) for run I-2 where NiO was insulated by mounting it on the mullite pellet.

Fig 7. XRD spectra of the reduced product when NiO is physically isolated from the current lead where (A) cathodic side (x), (B) anodic side (y) of run I-1, (C) outer part near the Ni basket and (D) central part of run I-2.

Fig 8. Scanning electron microscopic image (a) side (x), (b) side (y) of sintered sample from run I-1, (c) near the surface and (d) at the central part of product from run I-2.

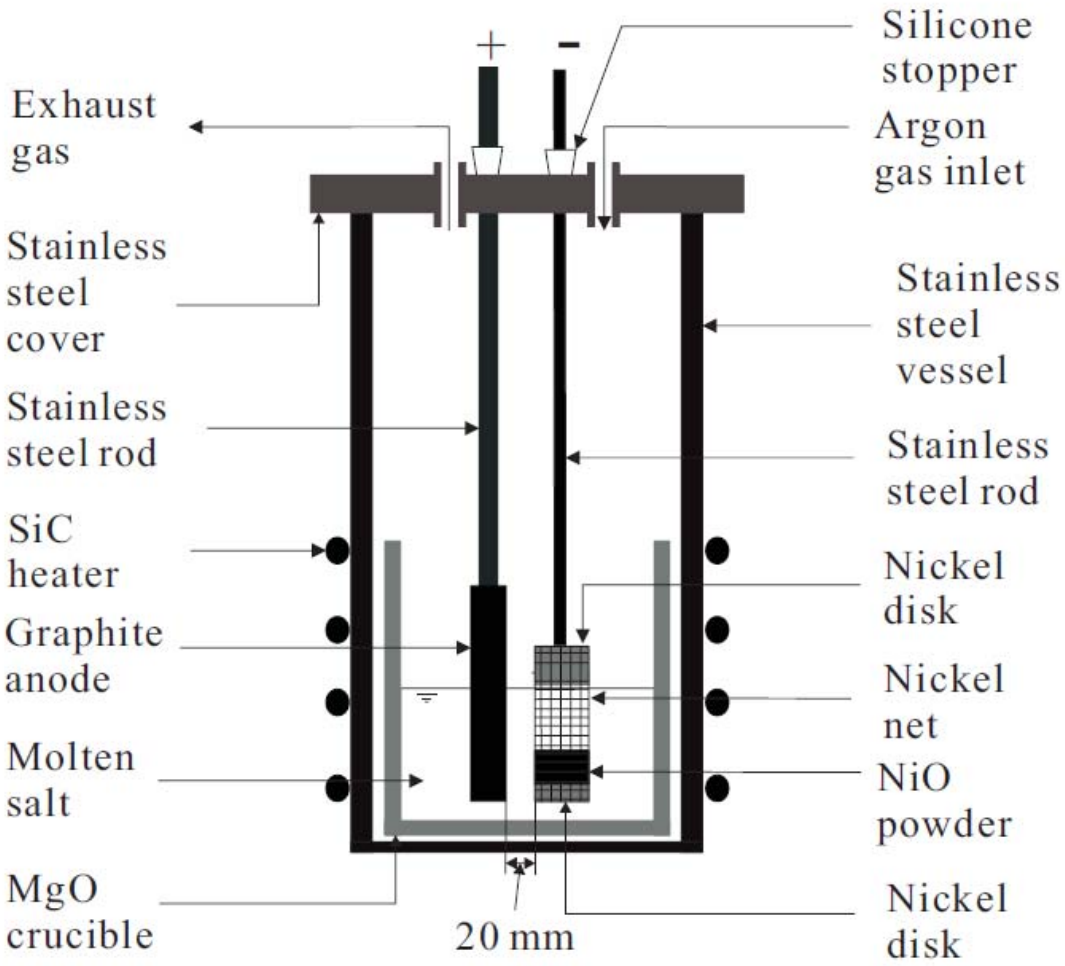

Fig. 1. Experimental apparatus for electrolysis.

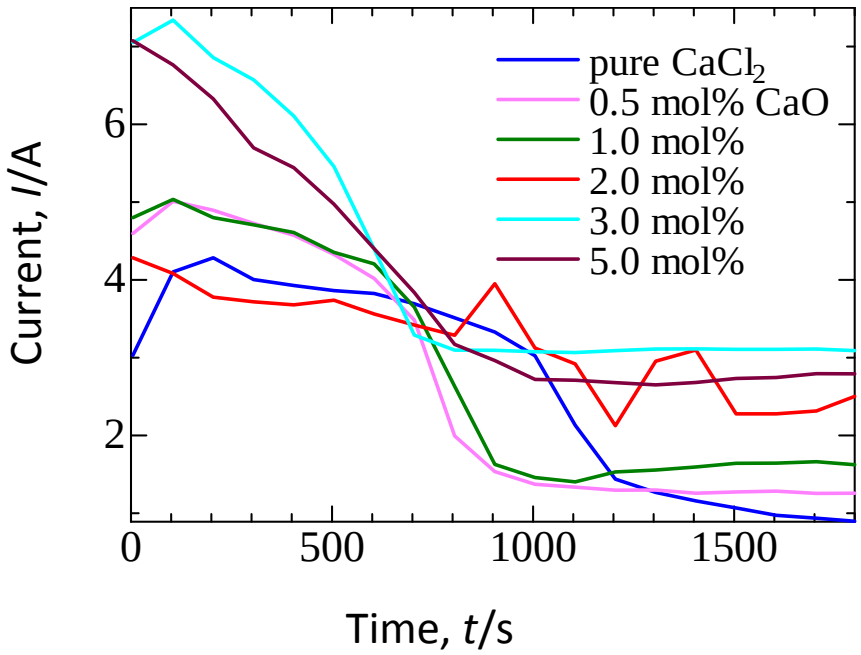

Fig. 2. Current versus time curves obtained during electrolysis for 1.8 ks at 1173 K with a constant potential of 3.1 V.

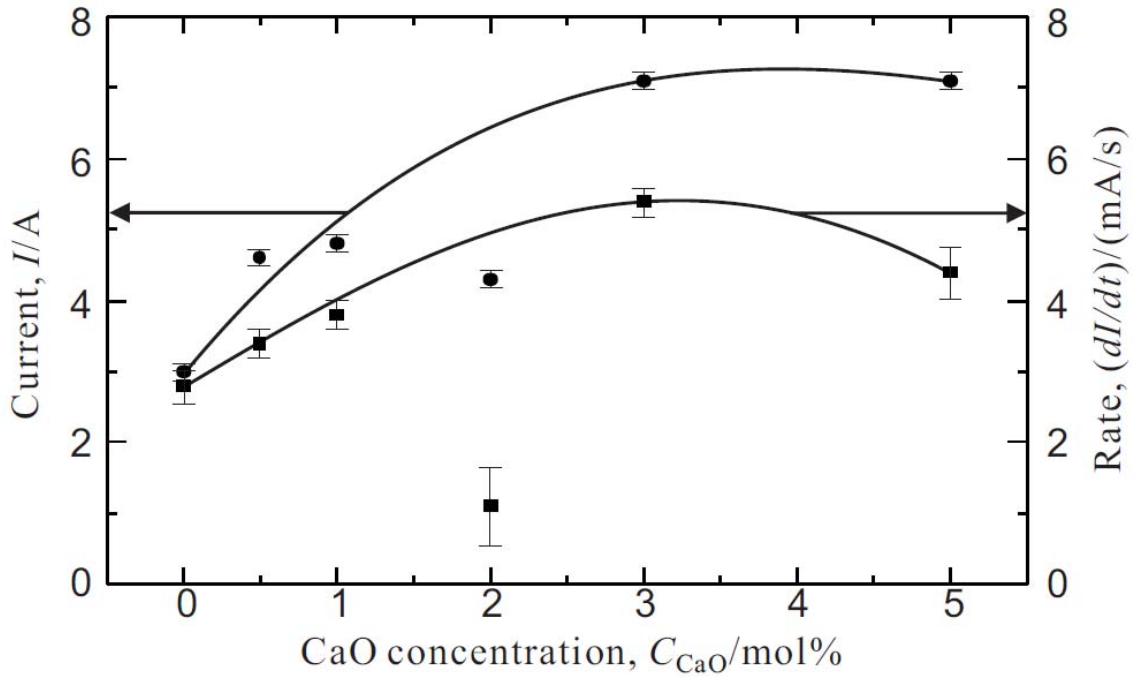

Fig. 3 The current reading at the start of electrolysis and the average slope of current decline.

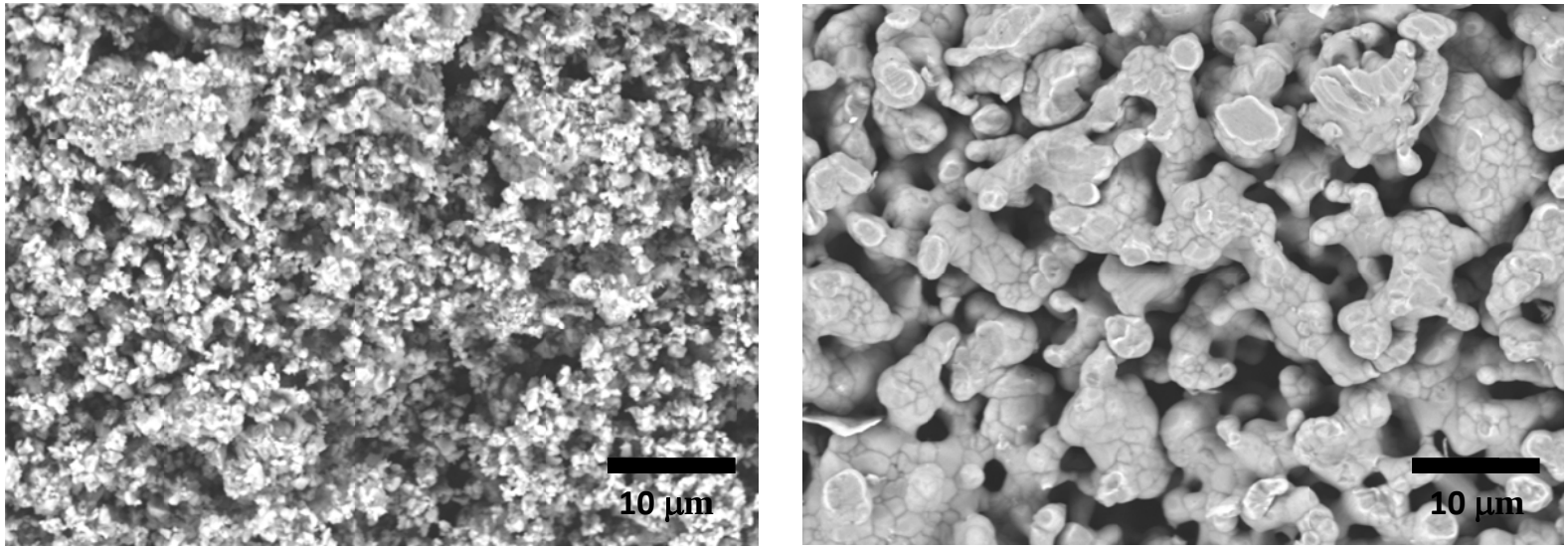

(a) (b)

Fig. 4. Scanning electron microscopic image of (a) starting NiO particles and (b) the sample reduced in a $CaCl_2$-1.0mol% CaO bath for 1.8 ks.

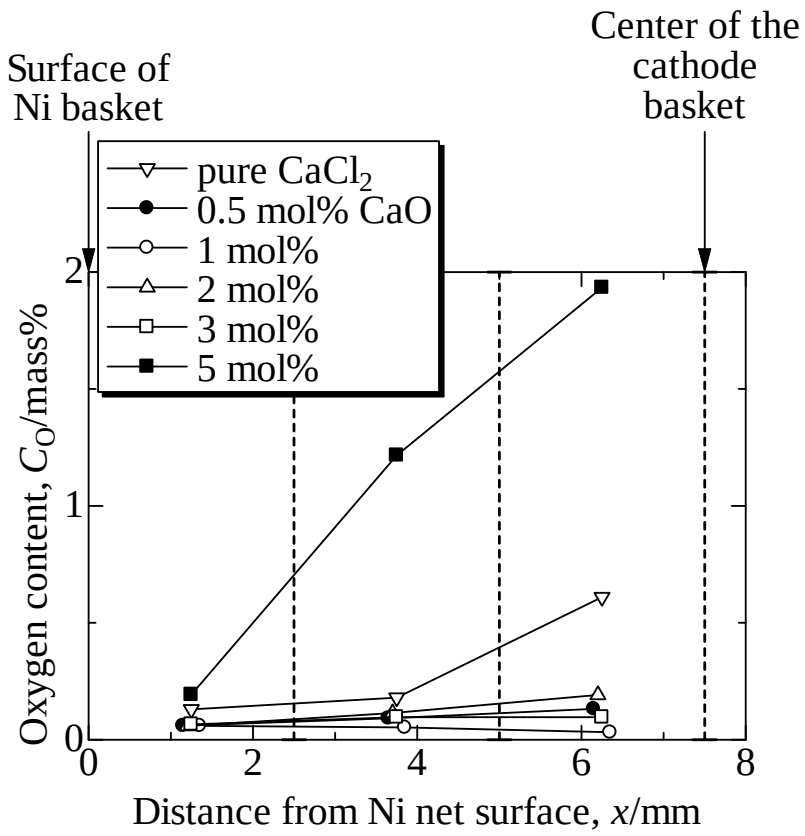

Fig. 5. Oxygen concentration distribution in the partially sintered samples.

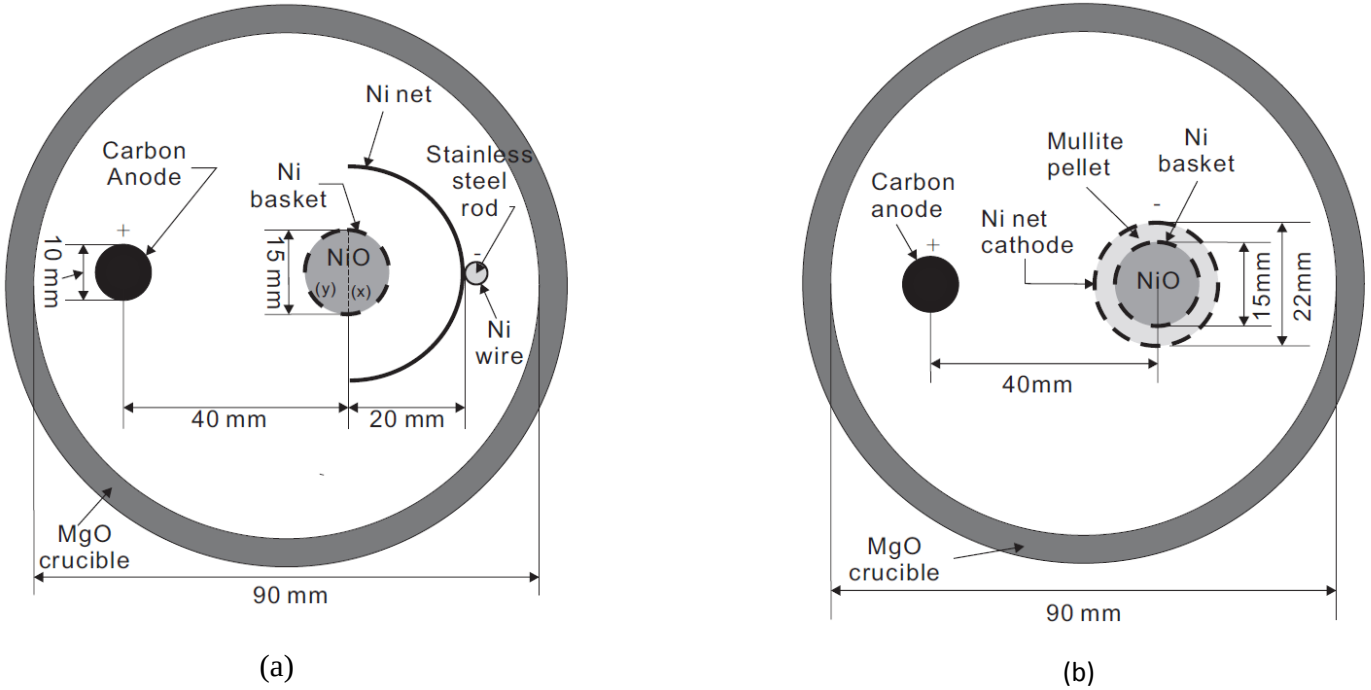

Fig. 6 Electrodes and NiO position during isolation experiment, (a) for run I-1 where NiO was placed in between the anode and cathode, and (b) for run I-2 where NiO was insulated by mounting it on the mullite pellet.

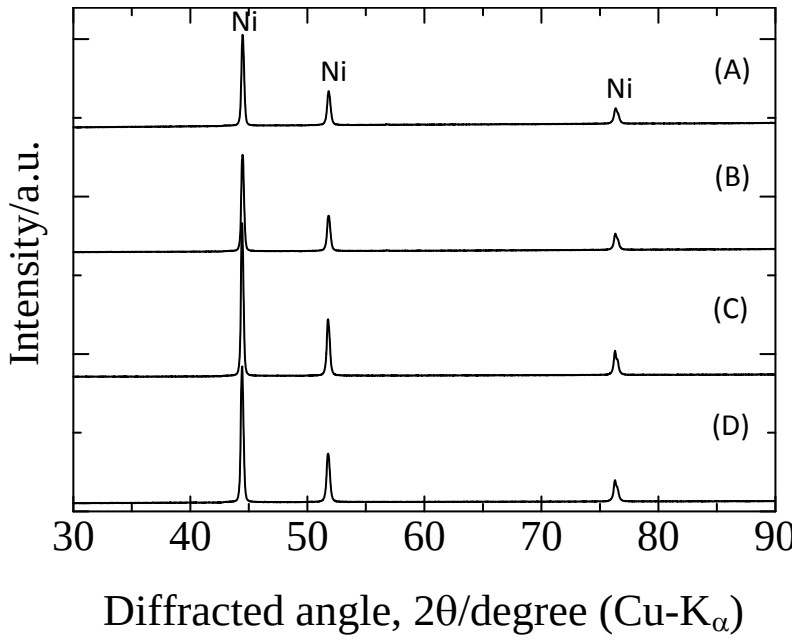

Fig. 7 XRD spectra of the reduced product when NiO is physically isolated from the current lead where (A) cathodic side (x), (B) anodic side (y) of run I-1, (C) outer part near the Ni basket and (D) central part of run I-2.

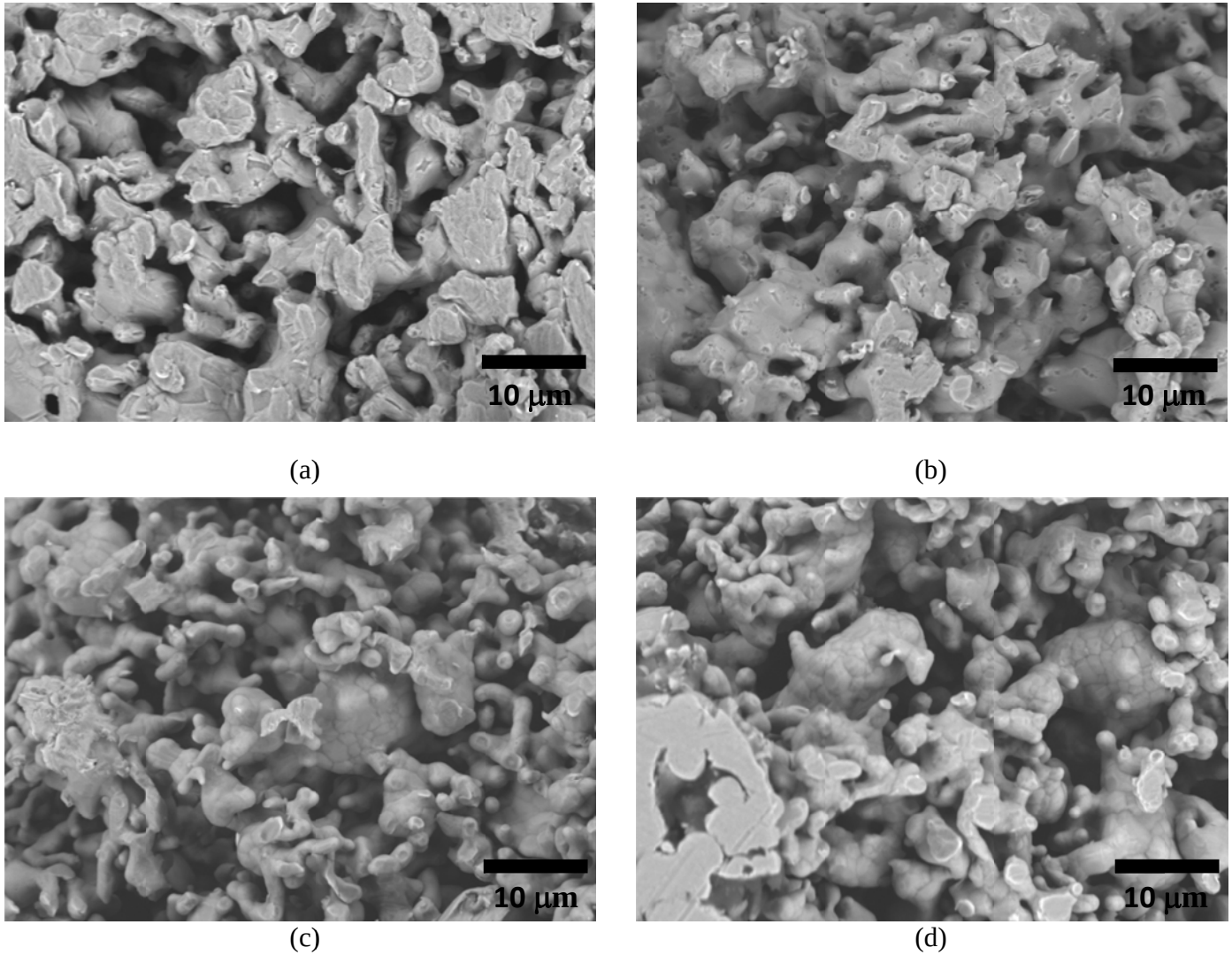

(a) (b)

(c) (d)

Fig. 8 Scanning electron microscopic image (a) side (x), (b) side (y) of sintered sample from run I-1, (c) near the surface and (d) at the central part of product from run I-2.

Table 1. Supplied charge, Q/Q_O, and phases identified by XRD when the samples were electrolyzed for 1.8 ks at 1173 K.

Run	Molten Salt (mol pct)	Charge (Q/Q_ox100%)	Phases Identified by XRD (distance from Ni net, mm) 0-2.5	2.5-5.0	5.0-7.5
1	$CaCl_2$	126.3	Ni	Ni, NiO(2 peaks)	Ni, NiO(3 peaks)
2	0.5 mol% CaO	129.5	Ni	Ni, NiO(1 peak)	Ni, NiO(2 peaks)
3	1.0 mol% CaO	138.3	Ni	Ni	Ni
4	2.0 mol% CaO	148.2	Ni	Ni	Ni, NiO(3 peaks)
5	3.0 mol% CaO	197.3	Ni	Ni	Ni
6	5.0 mol% CaO	182.3	Ni, NiO(2 peaks)	Ni, NiO(3 peaks)	Ni, NiO(5 peaks)

*In the measured range 5 diffraction peaks exist due to NiO. Because the existence of NiO was so small in the samples, the existence of NiO was identified only by several XRD peaks.

Table 2. Supplied charge, Q/Q_O, and phases identified by XRD when NiO was electrically isolated from the cathode. Electrolysis time was 10.8ks, applied voltage was 3.1 V and electrolysis temperature was 1173K.

Run	Charge (Q/Q_ox100%)	Residual Oxygen Content (ppm)		Phases Identified by XRD
I-1	366	side x	568	Ni[(1)]
		side y	597	Ni[(2)]
I-2	594	outer section	713	Ni[(3)]
		inner section	749	Ni[(4)]

[(1),(2),(3),(4)] XRD patterns are shown in Fig. 7 A,B,C and D, respectively.